11.5 Conclusions

Our present observations that estragole appears to be as potent an agonist of PPAR-alpha as clofibrate (on a $mg \cdot kg^{-1}$ basis) should now be confirmed by actual binding and signaling studies. If confirmed, the hepatocarcinogenic potential of this compound should be reevaluated accordingly. Although recent reports on estragole carcinogenicity suggest involvement of its metabolites[20] or glucocorticoid pathways,[21] our Percellome data support neither the involvement of such pathways or pronounced genotoxicity (which can be monitored indirectly as an enhancement in DNA repair and responses to oxidative stress). Interestingly, DEHP and Wyeth 14,643, well-characterized non-genotoxic rodent hepatocarcinogens that evoke tumors through peroxisome proliferation, gave mutation in Lac Z transgenic mice.[22]

Acknowledgements

The authors wish to thank Nae Matsuda, Kenta Yoshiki, Tomoko Ando, Noriko Moriyama, Yuko Kondo, Yuko Nakamura, Maki Abe, Ayako Imai, Koichi Morita, Shinobu Watanabe, Hisako Aihara, and Chiyuri Aoyagi for technical support. This study was supported financially by MHLW Health Sciences Research Grants H18-Kagaku-Ippan-001, H15-Kagaku-002, H14-Toxico-001, and H13-Seikatsu-012.

References

1. H. P. Rusch, B. E. Kline and C. A. Baumann, *Cancer Res.*, 1945, **5**, 431.
2. R. K. Boutwell, M. K. Brush and H. P. Rusch, *Cancer Res.*, 1949, **9**, 741.
3. D. Kritchevsky, M. M. Weber and D. M. Klurfeld, *Cancer Res.*, 1984, **44**, 3174.
4. J. Kanno, K. Aisaki, K. Igarashi, N. Nakatsu, A. Ono, Y. Kodama and T. Nagao, *BMC Genomics*, 2006, **7**, 64.
5. K.-I. Aisaki, 2011, in preparation.
6. J. M. Peters, R. C. Cattley and F. J. Gonzalez, *Carcinogenesis*, 1997, **18**, 2029.
7. S. S. Lee, T. Pineau, J. Drago, E. J. Lee, J. W. Owens, D. L. Kroetz, P. M. Fernandez-Salguero, H. Westphal and F. J. Gonzalez, *Mol. Cell. Biol.*, 1995, **15**, 3012.
8. S. Yu, W. Q. Cao, P. Kashireddy, K. Meyer, Y. Jia, D. E. Hughes, Y. Tan, J. Feng, A. V. Yeldandi, M. S. Rao, R. H. Costa, F. J. Gonzalez and J. K. Reddy, *J. Biol. Chem.*, 2001, **276**, 42485.
9. L. Billiet, C. Furman, C. Cuaz-Perolin, R. Paumelle, M. Raymondjean, T. Simmet and M. Rouis, *J. Mol. Biol.*, 2008, **384**, 564.
10. M. Rakhshandehroo, G. Hooiveld, M. Muller and S. Kersten, *PLoS One*, 2009, **4**, e6796.
11. C. B. Brocard, K. K. Boucher, C. Jedeszko, P. K. Kim and P. A. Walton, *Tra c*, 2005, **6**, 386.

12. C. Kural, H. Kim, S. Syed, G. Goshima, V. I. Gelfand and P. R. Selvin, *Science*, 2005, **308**, 1469.
13. D. T. Odom, N. Zizlsperger, D. B. Gordon, G. W. Bell, N. J. Rinaldi, H. L. Murray, T. L. Volkert, J. Schreiber, P. A. Rolfe, D. K. Gifford, E. Fraenkel, G. I. Bell and R. A. Young, *Science*, 2004, **303**, 1378.
14. H. Ren, L. M. Aleksunes, C. Wood, B. Vallanat, M. H. George, C. D. Klaassen and J. C. Corton, *Toxicol. Sci.*, **113**, 45.
15. J. G. Dekeyser, E. M. Laurenzana, E. C. Peterson, T. Chen and C. J. Omiecinski, *Toxicol. Sci.*, **120**, 381.
16. C. Xu, C. Y. Li and A. N. Kong, *Arch. Pharm. Res.*, 2005, **28**, 249.
17. G. A. Francis, E. Fayard, F. Picard and J. Auwerx, *Annu. Rev. Physiol.*, 2003, **65**, 261.
18. M. Lemoine, J. Capeau and L. Serfaty, *PPAR Res.*, 2009, **2009**, 906167.
19. FAO/WHO, 69th joint meeting, *Safety Evaluation of Certain Food Additives*, WHO Food Additives Series, International Programme on Chemical Safety, World Health Organization, Geneva, 2009.
20. Y. Ishii, Y. Suzuki, D. Hibi, M. Jin, K. Fukuhara, T. Umemura and A. Nishikawa, *Chem. Res. Toxicol.*, **24**, 532.
21. V. I. Kaledin, M. Y. Pakharukova, E. N. Pivovarova, K. Y. Kropachev, N. V. Baginskaya, E. D. Vasilieva, S. I. Ilnitskaya, E. V. Nikitenko, V. F. Kobzev and T. I. Merkulova, *Biochemistry (Moscow)*, 2009, **74**, 377.
22. M. E. Boerrigter, *J. Carcinog.*, 2004, **3**, 7.

Journal of Clinical and Experimental Medicine (IGAKU NO AYUMI)

[ISSN 0039-2359 CODEN:IGAYAY]

医学のあゆみ

第236巻・第12号 (通巻2843)
2011年3月19日発行 (毎週土曜日発行)
昭和21年7月27日第3種郵便物認可

Vol.236 No.12

2011
3/19

AYUMI

腎細胞癌の分子標的治療

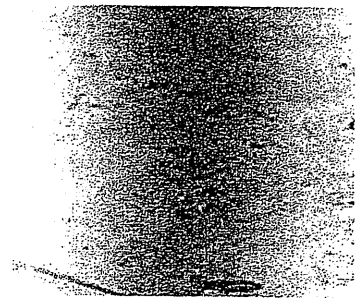

腎細胞癌の分子標的治療の理論的根拠
分子標的治療の時代におけるサイトカイン治療の位置づけ
転移性腎細胞癌におけるsorafenib治療の意義
血管新生阻害薬：sunitinib——腎細胞癌治療における有効性と問題点
mTOR阻害剤：everolimus
転移性腎癌に対するmTOR阻害薬：temsirolimus
Pazopanib——腎癌治療における位置づけ
第二世代の血管新生阻害薬：axitinib

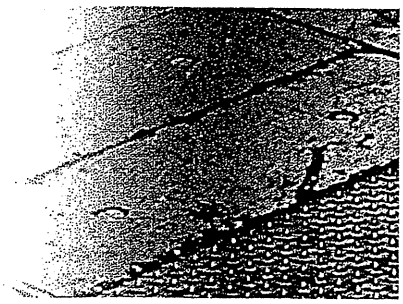

連載

動物の感染症から学ぶ
ヨーネ病——世界中に蔓延するウシの抗酸菌感染症

逆システム学の窓
あなたの職場の若者が結核排菌者と診断されたら
——患者へのサポートがDOTSを活かす

医歯薬出版株式会社
http://www.ishiyaku.co.jp/

医学のあゆみ Vol.236 No.12 2011/3/19

CONTENTS

AYUMI

腎細胞癌の分子標的治療

毒性学

Percellomeトキシコゲノミクスの進捗

Progress in percellome toxicogenomics

Percellomeトキシコゲノミクスプロジェクトとは

2006年に本誌の当欄にて，毒性学の高精度解析手法として開始した“Percellomeトキシコゲノミクスプロジェクト”を紹介させていただいた[1]．当毒性部の基本姿勢は変わらず，さまざまな物質が身体に取り込まれた際に生じる可能性のある毒性(有害性)を予測し，それらの使用に際しての被害を未然に防ぐのが毒性学の役割であるとの考えに立脚し，身のまわりにあり，体のなかに入ってくるすべての“もの”について，どのような場合に(胎児・新生児・小児など，吸い込む・飲み込むなど)，どのくらいの量で，どのような症状が現れるか(急性毒性，発癌を含む慢性毒性，遅発性毒性など)について研究を継続している．

具体的には実験動物の診断所見をヒトに外挿すべく実施しているが，従来法では種差や個体差は“安全係数”により量的な安全マージンをとることで勘案されてきた．しかし，サリドマイド奇形に代表されるように，これには科学的な限界があり，“毒性学の近代化”が必要である．医薬品の場合はヒトで治験を行える場合があるが，それも胎児や新生児には実施困難であり，一般的な物質の毒性を検討することを考えると現状では動物実験は不可避である．そこで，著者らはヒトの身代りとしての実験動物(遺伝子改変動物の活用を含む)を対象とした，Percellomeトキシコゲノミクス研究を開始した次第である．

これは生体というブラックボックスの中身を遺伝子発現ネットワークの面から解明することにより，生体反応メカニズムに基づいた分子毒性学を構築することを目的としている．その際，毒性を見落とさない“網羅性”を確保する必要性から，全遺伝子のトランスクリプトーム情報のなかから生物学的に有意と判断される反応ネットワークを網羅的に抽出するアプローチをとっている．複数の実験から得られる大量のデータを蓄積し横断的な解析を加えることが必須であることから，マイクロアレイデータの標準化と互換性確保のために“細胞1個当りのmRNAコピー数”を得るPercellome法[2]を開発し，プロジェクトを軌道に乗せたところまでを前回の記事でご紹介した．

最近の展開

その後の数年間に，100種類超(医薬品，一般化学物質，食品関連物質を含む)の化学物質によるマウス肝の初期応答データを含む，延べ3.5億遺伝子情報からなるPercellomeデータベースを得た．これは，基本的に投与後の時間，曝露用量，遺伝子発現量の3軸からなる三次元曲面データにより構成される(図1)．解析には，この三次元曲面の特徴抽出という独創的な方法をとり，解析ソフトウェア群(相崎健一ら)は独自開発である．また，動物実験レベルからのシステム管理により，高精細かつ高再現性を実現している．

得られたデータの例としては，アリル炭化水素受容体(AhR)に結合するダイオキシン(2, 3, 7, 8-TCDD)が比較的少数のAhR直下の遺伝子の発現を2時間目に誘導し，4, 8, 24と時間が経過する

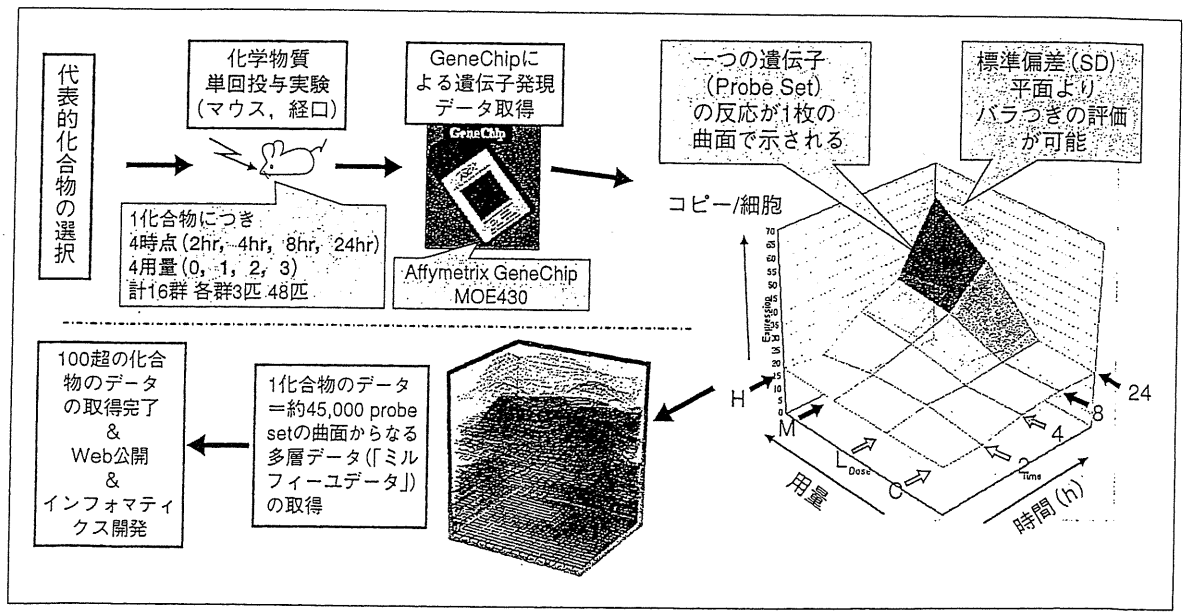

図1　Percellomeデータベースの概要

につれ数を増す状況が確認された．ダイオキシンの体内半減期が25時間であるにもかかわらず，2時間目のみの一過性発現のパターンをとるもの，持続的に発現が増加するものなどが観測されている．シックハウス症候群の指針値程度の，ごく低濃度域での吸入毒性トキシコゲノミクスも実施しており，ごく低濃度のホルマリン(0.1 ppm 付近)で肺の複数の遺伝子発現が明確に誘導されることをみている．サリドマイドは近年，癌治療薬として使用されていることから，複数の臓器における初期誘導を観測したところ，肺の2時間目に用量相関性をもって発現誘導のピークを示す遺伝子に，Cdkn1a (P21)が認められた．類似の発現パターンを示す初期応答遺伝子には，Fas，Foxo3a，Gata2など50あまりがあり，酸化的ストレスが誘発されることが推測された．実際，癌患者にサリドマイドが間質性肺炎を誘発する報告が増加しており，ヒトで確認された形となっている．

また，Percellomeトキシコゲノミクスを発生毒性へも適用している．妊娠マウスにサリドマイドを投与し胎児で発現変動が認められた遺伝子のなかに，マウス胚の肢部形成に重要な分子が見出され(その遺伝子をノックアウトしたマウス胚にアザラシ肢症に類似の奇形が生じる)，サリドマイド奇形の標的分子検索の糸口が示唆された．さらに，胎生期～幼若期の発達中の脳に対する神経シグナル撹乱が脳構造や神経回路の形成に影響を及ぼし，成熟後に行動異常などの脳高次機能の障害として顕在化することを見出している．これについては，妊娠マウスへ神経伝達物質類似物質を投与し，生まれたマウスに誘発される遅発性中枢毒性と海馬の遺伝子発現異常の関連解析から標的ネットワークが示唆されつつある．

このほかにも投与した化学物質に関して，いままで報告のないあらたな遺伝子発現変動現象を多数見出し，そのいくつかには特定の毒性との連鎖を示唆する分子生物学的情報がみつかっていることから，それらを順次報告および一般公開する準備を進めている(http://www.nihs.go.jp/tox/TTG_Archive.htm；現在更新中．2010年度中再開予定)．

プロジェクトの今後

さらに，マイクロアレイのクロスハイブリダイゼーションを修正するアルゴリズムの開発を終え(特許出願準備中)，その実装準備中である(NTTデータおよび日本テラデータとの委託共同研究)．また，遺伝子ネットワークと毒性の動的な因果関係を導き出すインフォマティクスの構築研究やPercellomeデータの統合的提示方法の開発にも本格的に取り組んでおり(ソニーコンピュータサイエンス研究所との共同研究)，段階的に皆様にご披露できる予定である(厚生労働科学研究費補助金，環境研究総合推進費などによる)．

1) 菅野　純：毒性の高精細解析に向けてのトキシコゲノミクス．医学のあゆみ，218：1035-1036，2006．
2) Kanno, J. et al.："Per cell" normalization method for mRNA measurement by quantitative PCR and microarrays. *BMC Genomics*, 7：64, 2006.

菅野　純／Jun KANNO
国立医薬品食品衛生研究所
安全性生物試験研究センター毒性部

循環器内科学

心筋トロポニンの高感度測定の有用性

Clinical utility of high-sensitivity cardiac troponin assay

従来の心筋トロポニン測定は検出感度が低いため，急性冠症候群の診療以外で用いられることはまれであった．最近，検出感度が5倍以上改善された高感度測定が臨床の場に登場した．この高感度測定は，従来測定では検出不可能であった小さな心筋障害を診断できる．そのため，超急性期の心筋梗塞診断の精度[1,2]や慢性心不全における予後予測の精度[3]を高めることが示されている．さらに，外来診療や検診・人間ドック分野へのあらたな展開も期待される．

急性冠症候群の診療

トロポニンが上昇している不安定狭心症は，突然死や急性心筋梗塞発症の危険度が高い．このトロポニンの上昇は，破砕したプラークや血栓が引き起した末梢の微小塞栓による微小心筋障害を反映している．そのため，2000年に公表されたヨーロッパ心臓病学会/アメリカ心臓病学会(ESC/ACC)の心筋梗塞の再定義[4]は，トロポニンが上昇している不安定狭心症を急性心筋梗塞に包括した．さらに，ヨーロッパ心臓病学会/アメリカ心臓病学会/アメリカ心臓協会/世界心臓協会(ESC/ACC/AHA/WHF)の共同タスクフォースは，2007年に急性心筋梗塞の診断基準の再改定[5]を公表した．新しい診断基準では，トロポニンの心筋梗塞診断における基準値を健常人の99thパーセンタイル値より大と定めた．一般に，測定値の相対的なばらつき(変動係数．coefficient of variation：CV)が小さいほど測定値の精度は高い．共同タスクフォースは試薬の精度にも言及しており，健常人の99thパーセンタイル値における変動係数が10%以下である試薬を用いることを推奨した．従来の試薬はこの条件を

The Journal of Toxicological Sciences (J. Toxicol. Sci.)
Vol.37, No.2, 373-380, 2012

Original Article

Development of humanized steroid and xenobiotic receptor mouse by homologous knock-in of the human steroid and xenobiotic receptor ligand binding domain sequence

Katsuhide Igarashi[1], Satoshi Kitajima[1], Ken-ichi Aisaki[1], Kentaro Tanemura[1], Yuhji Taquahashi[1], Noriko Moriyama[1], Eriko Ikeno[1], Nae Matsuda[1], Yumiko Saga[2,3], Bruce Blumberg[4] and Jun Kanno[1]

[1]Division of Cellular and Molecular Toxicology, Biological Safety Research Center, National Institute of Health Sciences, 1-18-1 Kamiyoga, Setagaya-ku, Tokyo, 158-8501, Japan
[2]Division of Mammalian Development, National Institute of Genetics, Yata 1111, Mishima 411-8540, Japan
[3]The Graduate University for Advanced Studies (Sokendai), Yata 1111, Mishima 411-8540, Japan
[4]Department of Developmental and Cell Biology, 2011 Biological Sciences 3, University of California, Irvine, CA 92697-2300, USA

(Received December 7, 2011; Accepted January 12, 2012)

ABSTRACT — The human steroid and xenobiotic receptor (SXR), (also known as pregnane X receptor PXR, and NR1I2) is a low affinity sensor that responds to a variety of endobiotic, nutritional and xenobiotic ligands. SXR activates transcription of Cytochrome P450, family 3, subfamily A (CYP3A) and other important metabolic enzymes to up-regulate catabolic pathways mediating xenobiotic elimination. One key feature that demarcates SXR from other nuclear receptors is that the human and rodent orthologues exhibit different ligand preference for a subset of toxicologically important chemicals. This difference leads to a profound problem for rodent studies to predict toxicity in humans. The objective of this study is to generate a new humanized mouse line, which responds systemically to human-specific ligands in order to better predict systemic toxicity in humans. For this purpose, the ligand binding domain (LBD) of the human SXR was homologously knocked-in to the murine gene replacing the endogenous LBD. The LBD-humanized chimeric gene was expressed in all ten organs examined, including liver, small intestine, stomach, kidney and lung in a pattern similar to the endogenous gene expressed in the wild-type (WT) mouse. Quantitative reverse transcription-polymerase chain reaction (RT-PCR) analysis showed that the human-selective ligand, rifampicin induced Cyp3a11 and Carboxylesterase 6 (Ces6) mRNA expression in liver and intestine, whereas the murine-selective ligand, pregnenolone-16-carbonitrile did not. This new humanized mouse line should provide a useful tool for assessing whole body toxicity, whether acute, chronic or developmental, induced by human selective ligands themselves and subsequently generated metabolites that can trigger further toxic responses mediated secondarily by other receptors distributed body-wide.

Key words: Steroid and xenobiotic receptor, Pregnane X receptor, Humanized mouse, Ligand binding domain, Knock-in mouse

INTRODUCTION

Most orally administered xenobiotics are metabolized first by the intestine and then by the liver after portal transport. The expression levels of enzymes involved in xenobiotic metabolism are regulated at the transcriptional level by key xenobiotic sensors including the steroid and xenobiotic receptor (SXR), also known as the pregnane X receptor (PXR), pregnane activated receptor (PAR) and NR1I2 (Bertilsson *et al.*, 1998; Lehmann *et al.*, 1998; Blumberg *et al.*, 1998). SXR is important in the field of toxicology for at least two reasons. Firstly, this receptor system induces the expression of CYP3A and CYP2B enzymes, the major metabolizers of pharmaceu-

Correspondence: Jun Kanno (E-mail: kanno@nihs.go.jp)

ticals and xenobiotics. Therefore, SXR is a key mediator of drug- and chemical-induced toxicity as well as drug-drug and drug-nutrient interactions (Zhou *et al.,* 2004). Secondly, the orthologous rodent and human receptors exhibit differential sensitivity for a subset of chemical ligands important in the field of toxicology. For example, rifampicin (RIF) is a specific and selective activator of human SXR, whereas pregnenolone 16a-carbonitrile (PCN) is selective for the rodent orthologue.

Rodent-human differences in CYP3A and CYP2B-mediated responses to xenobiotics can be a profound problem in toxicologic studies where rodents are used to predict the toxicity of a compound in humans (Ma *et al.*, 2007). Therefore, development of a murine model that reconstructs the SXR-mediated systemic response of humans is of a great significance in toxicology.

Human and rodent SXRs share ~95% amino acid sequence identity in the DNA-binding domain (DBD) but only about 77% identity in the LBD. Tirona *et al.* (2004) analyzed the ligand selectivity of a human-rat chimeric protein and showed that the species differences are primarily defined by sequence differences in the LBD. Watkins and colleagues showed that the key residues responsible for the majority of the ligand selectivity were Leu 308 (human) and Phe305 (rat and mouse). Crystallographic analysis located these amino acids within or neighboring the flexible loop that forms a part of the pore to the ligand-binding cavity. Swapping the rodent and human-specific residues was shown to modulate the activation by the human-selective activator RIF *in vitro* (Watkins *et al.*, 2001). According to those findings, a simple replacement of the mouse LBD with the human sequence should be sufficient to "humanize" the ligand binding properties as well as activation of the downstream target genes.

Three kinds of humanized mice have already been generated. One is the SXR-null/Alb-SXR mouse (Alb-SXR mouse) made by crossing the SXR knockout mice with a transgenic mouse line that expresses human SXR in liver under the control of the albumin promoter (Xie *et al.*, 2000). Gonzalez and colleagues generated a transgenic mouse expressing a human BAC containing the entire hSXR gene in a SXR null background, thus controlled under human SXR promoter (SXR BAC mouse) (Ma *et al.*, 2007). Another mouse is the human SXR genome knock-in mice (hSXR genome mouse) (Scheer *et al.*, 2008). The human SXR genomic region from exon 2 to exon 9 was knocked-in to mouse SXR exon 2. This mouse expresses the human full length SXR mRNA under the control of mouse SXR promoter regulation. Although useful for toxicology studies, these mice have disadvantages in that the human SXR is expressed only in the liver (Alb-SXR mouse), hSXR mRNA is not expressed in all of the tissues where SXR is known to be expressed (SXR BAC mouse), and there might be potential differences in the binding affinities of hSXR DNA-binding domain (DBD) to *cis*-acting elements in mouse SXR target genes (hSXR genome mouse).

As noted above, it is known that the critical differences between human and rodent ligand-selectivity reside in the LBD. Therefore, when our project to generate a humanized SXR mouse was initiated, we reasoned that altering the LBD would be sufficient to generate a humanized ligand selectivity. We decided to retain the mouse DBD to avoid any potential differences between the binding affinities of the chimeric receptor for cis-acting elements in the mouse genome. To maintain the tissue-specific expression pattern of the endogenous gene, we inserted the human cDNA encoding the region carboxyl-terminal to the DBD into the mouse gene. This retains all of the 5' and 3' regulatory elements in the mouse gene, as well as introns 1 and 2, which contain important elements for regulating SXR expression (Jung *et al.*, 2006).

Here we report a new line of mouse (hSXRki mouse) in which a cDNA encoding the human LBD is homologously recombined into the mouse gene after exon 3. The tissue distribution of the resulting chimeric mouse DBD-human LBD mRNA is comparable to that of the WT mouse. The hSXRki mouse showed a fully humanized response to the human-selective activator RIF in that the Cyp3a11 mRNA was induced in liver and mucosa of small intestine in response to RIF, but not the rodent-selective compound PCN. This new mouse line should provide a useful tool for assessing the whole body toxicity induced by a human selective SXR ligand itself and its subsequently generated metabolite(s) that can trigger further toxic responses through other pathways body-wide.

MATERIALS AND METHODS

Generation of hSXRki knock-in mice

A DNA fragment of mouse SXR intron 2 to exon 3 was PCR amplified using mouse BAC DNA (BAC clone No. RP23-351P21) as a template. Primers used were BAC39486FW and mSXR462RV (for sequences of the primers see Table1). This fragment was connected to the LBD of human SXR cDNA from amino acid 105 through the carboxyl terminus amplified by the PCR primers: hSXR904FW and hSXR1887RVEcoRI (template; human SXR cDNA). The 3'UTR of bovine growth hormone (BGH) was added to 3' to the terminal codon. This concatenated fragment was introduced to a vector, which

Table 1. List of primer pairs

Purpose	Primer name	Sequence (5' to 3')
Targeting vector construction	BAC39486FW	CCATGGGTACCACGAATAACAA
	mSXR462RV	CATGCCACTCTCCAGGCA
	hSXR904FW	AAGAAGGAGATGATCATGTCCG
	hSXR1887RVEcoRI	CCGAATTCTCATCATCAGCTACCTGTGATACCGAACA
Genotyping	NeoAL2	GGGGATGCGGTGGGCTCTATGGCTT
	SXR RC RV5	TGAGAGTGCACAAGTTCAAGCT
	WTInt5	AGTGATGGGAACCACTCCTG
	WTEx6RV	TGGTCCTCAATAGGCAGGTC
	mhSXRE4	GTGAACGGACAGGGACTCAG
	mhSXRSARV	CTCTCCTGGCTCATCCTCAC
Percellome quantitative RT-PCR	Cyp3a11 FW	CAGCTTGGTGCTCCTCTACC
	Cyp3a11 RV	TCAAACAACCCCCATGTTTT
	Ces6 FW	GGAGCCTGAGTTCAGGACAGAC
	Ces6 RV	ACCCTCACTGTTGGGGTTC
	mouse SXR FW	AATCATGAAAGACAGGGTTC
	mouse SXR RV	AAGAGCACAGATCTTTCCG
	human SXR FW	ATCACCCGGAAGACACGAC
	human SXR RV	AAGAGCACAGATCTTTCCG
	mouse-human SXR FW	CCCATCAACGTAGAGGAGGA

has the neomycin resistance gene with loxP sequence at both ends, removable with Cre recombinase (Saga *et al.*, 1999). A 7kb KpnI fragment containing intron 2 was used as a long arm and 1.3kb PstI-EcoRI fragment containing from exon 8 to intron 8 was used as a short arm for homologous recombination (Fig. 1). The resulting targeting vector was linearized with SacII and introduced by electroporation to TT2 ES cell line (Yagi *et al.*, 1993) and neomycin resistant clones were selected, PCR genotyped, and confirmed by the Southern blotting. For generation of chimeric mice, these ES clones were aggregated with ICR 8-cell embryos and transferred to pseudopregnant female recipients. The chimeric mice born were bred with ICR females. Germ line transmission of the targeted allele was confirmed by PCR. A mouse was crossed with a CAG-Cre transgenic mouse (Sakai and Miyazaki, 1997) to evict the neomycin resistance gene, and back crossed to C57BL/6 CrSlc (SLC, Inc., Shizuoka, Japan) at least 6 generations and used for the analysis.

PCR Genotyping (See Table 1 for primer sequences)

Primers for identification of homologously recombined ES clones were NeoAL2 and SXR RC RV5. DNA purified from the tail of each mouse was used for PCR genotying. Primers for WT detection were WTInt5 and WTEx6RV amplifying a product of 755 bp. Primers for confirmation of removal of the neomycin resistance gene were mhSXRE4 and mhSXRSARV amplifying a product of 1,223 bp.

Southern blot analysis

To confirm homologous recombination, DNA from ES cell cultures was purified and digested with BamHI and XhoI, then electrophoresed and analyzed by Southern hybridization (Saga *et al.*, 1997). Mouse SXR exon 9 region which remains after homologous recombination was used for the probe. The restriction fragments from the WT allele and targeted allele are 2,305 bp and 1,925 bp, respectively.

Chemicals

RIF (molecular weight 822.95) and PCN (molecular weight 341.49) were purchased from Sigma-Aldrich (St. Louis, MO, USA). Corn oil was purchased from Wako Pure Chemical Industries (Osaka, Japan).

Quantitative RT-PCR (Percellome PCR) (See Table 1 for primer sequences)

The method for Percellome quantitative RT-PCR was described previously (Kanno *et al.*, 2006). Briefly, tissue pieces stored in RNAlater (Ambion, Austin, TX, USA) were homogenized and lysed in RLT buffer (Qiagen GmbH., Germany) and 10 μl aliquots were used

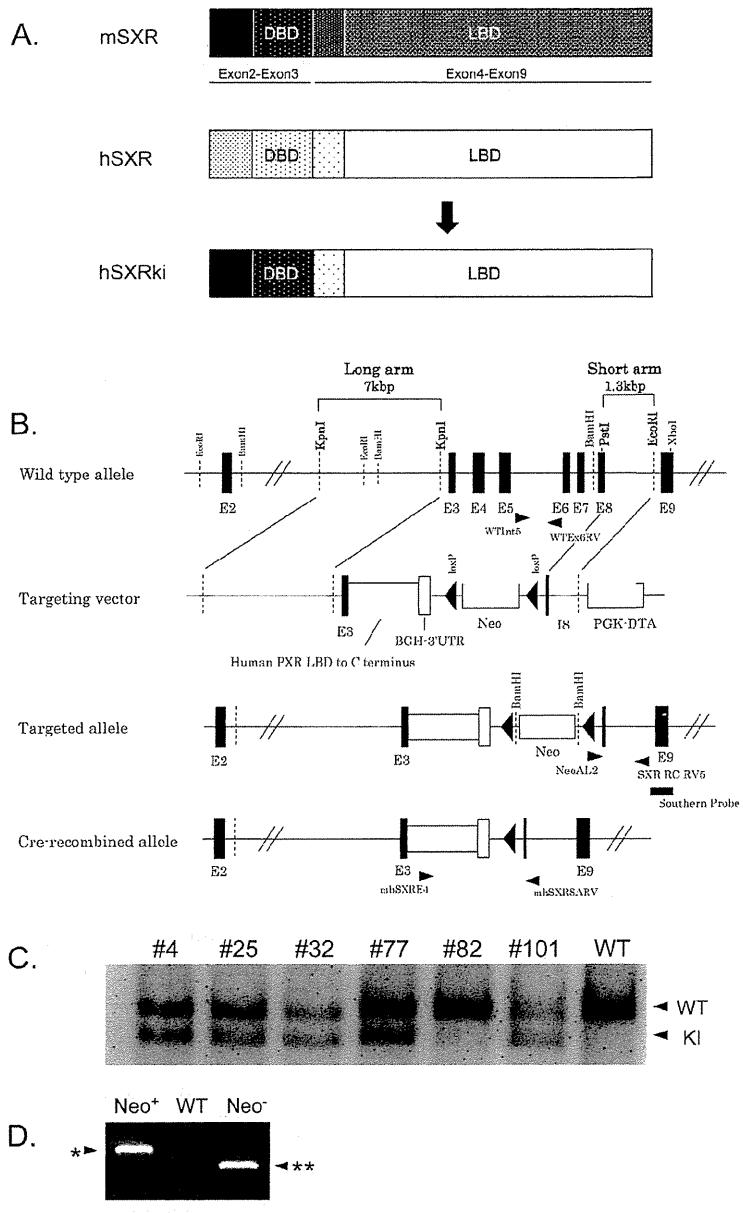

Fig. 1. Targeting strategy used to generate the hSXRki mouse. A) Diagram of hSXRki chimeric protein. Hinge region and ligand binding domain (LBD) of human SXR are knocked-in to mouse SXR, resulting in chimeric protein having murine N-ternial domain and DNA binding domain (DBD). B) Targeting strategy used to generate the hSXRki mouse. The chimeric mouse DBD and human LBD fragment, followed by the BGH 3' UTR were knocked-in to the mouse SXR gene. The genomic region spanning from exon 3 to exon 8 was substituted by the inserted fragment with the remainder of the gene remaining intact. C) Confirmation of homologous recombination by southern blot analysis. Six ES clones positive for recombination by PCR genotyping were further analyzed by southern blot (clones #4 ~ #101). Lower bands (1925 bp) indicate successful homologous recombination; upper bands (2305 bp) correspond to WT allele. Clones #4, #25, #32, #77 and #101 were confirmed as homologous recombinants; clones #4 and #25 were used for the generation of chimeric mice. D) Confirmation of Cre-mediated removal of the neomycin resistance gene. Mouse tail genome DNA was PCR amplified with the primer set, mhSXRE4 and mhSXRSARV. *: 2,858 bp (for the mice having the neomycin resistance gene), **: 1,223 bp (for the mice without the neomycin resistance gene).

for genomic DNA quantification with PicoGreen fluorescent dye (Invitrogen, Carlsbad, CA, USA). A prepared spike mRNA cocktail solution containing known quantity of five mRNAs of bacillus subtilis was added to the tissue lysate in proportion to the DNA quantity. Total RNA was purified from the lysate using the RNeasy kit (Qiagen). One microgram of total RNA was reverse-transcribed with SuperScript II (Invitrogen). Quantitative real time PCR was performed with an ABI PRISM 7900 HT sequence detection system (Applied Biosystems) using SYBR Green PCR Master Mix (Applied Biosystems), with initial denaturation at 95°C for 10 min followed by 40 cycles of 30 sec at 95°C and 30 sec at 60°C and 30 sec at 72°C, and Ct values were obtained. Primers for Cyp3a11 were Cyp3a11 FW and Cyp3a11 RV. Primers for Ces6 were Ces6 FW and Ces6 RV. Primers for mouse SXR selective quantification were mouse SXR FW and mouse SXR RV. Primers for hSXRki selective quantification were human SXR FW and human SXR RV. Primers for both mouse SXR and hSXRki quantification were mouse-human SXR FW and mouse-human SXR RV that amplify the DBD region of the chimera.

In Situ Hybridization analysis

Digoxigein-labeled cRNA probe for Cyp3a11 was synthesized according to Suzuki *et al.* (2005) by RT-PCR using mouse liver cDNA as a template. The primers used were as follows: forward 5'-GATTGGTTTTGATGCCTGGT-3' and reverse 5'-CAAGAGCTCACATTTTTCATCA-3'. The amplified product was sequence confirmed and ligated with Block-iT T7-TOPO (Invitrogen) Linker, which contains the T7 promoter site. A secondary PCR was performed to generate the sense and antisense DNA templates. For antisense template, Block-iT T7 Primer and Cyp3a11 forward primer (or reverse primer for generation of sense DNA template), the same primer as for the first PCR amplification, were used. With these DNA templates, both sense and antisense digoxigenin-labeled riboprobes were synthesized using a DIG RNA labeling kit (Roche Diagnostics, Germany) according to the manufacturer's protocol.

ISH on paraffin sections was carried out according to Suzuki *et al.* with a modification; permeabilization condition 98°C for 15 min in HistoVT One (Nacalai tesque, Japan).

Animals experiments

Male hSXRki and WT mice were maintained under a 12 hr light/12 hr dark cycle with water and chow (CRF-1, Oriental Yeast Co. Ltd., Tokyo, Japan) provided *ad libitum*. The animal studies were conducted in accordance with the Guidance for Animal Studies of the National Institute of Health Sciences under Institutional approval. The expression level of the hSXRki and WT SXR mRNA of ten organs (brain, thymus, heart, lung, liver, stomach, spleen, kidney, small intestine and testis) were analyzed on 15 weeks old male mice (n = 2) by the Percellome quantitative RT-PCR.

For the demonstration of selective gene induction by RIF and PCN in hSXRki and WT male mice on 13 weeks

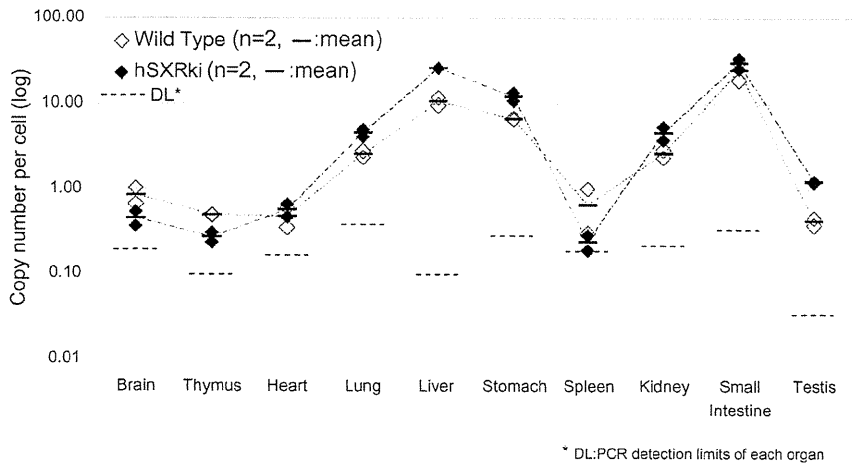

Fig. 2. Conservation of tissue expression patterns of hSXRki mRNA in the knock-in mouse. Percellome quantitative RT-PCR analysis was performed to measure the absolute expression levels of WT SXR mRNA and hSXRki mRNA in ten organs of WT and hSXRki mice. The expression levels of hSXRki mRNA among organs were comparable to WT.

old, three mice per group were singly dosed orally with vehicle (corn oil+0.1% DMSO), 10, 30, or 100 mg/kg of RIF, or 20, 70, or 200 mg/kg PCN (approximately equivalent in molar dose). Eight hours later, mice were sacrificed by exsanguination under ether anesthesia and the liver and the small intestine mucosa were sampled. Liver samples in small pieces were stored in RNA later (Applied Biosystems, Foster City, CA, USA) for further analysis. The small intestine under ice-cooled condition was longitudinally opened, gently rinsed with RNase-free saline and the epithelium was scraped with a glass slide and immersed in RNAlater. For *in situ* hybridization (ISH) of Cyp3a11 in the liver, 15 weeks old male hSXRki and WT mice were dosed orally with vehicle (corn oil), RIF (10 mg/kg), or PCN (40 mg/kg) daily for 3 days and liver sampled 24 hr later. All mice were sacrificed by exsanguination under ether anesthesia.

Statistical analysis

All values are expressed as the means ± S.D. and group differences analyzed by unpaired Student's *t* test or one-way ANOVA followed by Dunnett's post hoc comparison. Level of significance was set at $p < 0.05$.

RESULTS

Generation of hSXRki knock-In mice

Among 144 neomycin resistant TT2 ES clones, six PCR positive clones were further submitted to Southern blotting for the confirmation of homologous recombination. As shown in Fig. 1C, five clones were confirmed, and two (#4 and #25) were used to generate chimeric mice. The resulting mice were backcrossed to ICR strain to confirm germline transmission. One clone (#4) was crossed to a mouse constitutively expressing Cre recombinase to remove the neomycin resistance gene (Fig. 1D) and backcrossed to C57BL/6 CrSlc for at least 6 generations before further analysis.

Tissue distribution of hSXRki mRNA

Ten tissues, i.e., brain, thymus, heart, lung, liver, stomach, spleen, kidney, small intestine and testis from both hSXRki and WT mice were measured for hSXRki or WT SXR mRNA expression by the Percellome quantitative RT-PCR. As shown in Fig. 2, the levels of hSXRki mRNA are comparable to that of SXR in WT mouse and expressed in all tissues analyzed.

Humanized responses in hSXRki mouse

Humanized response of hSXRki was demonstrated by administration of the mouse-specific ligand PCN and the

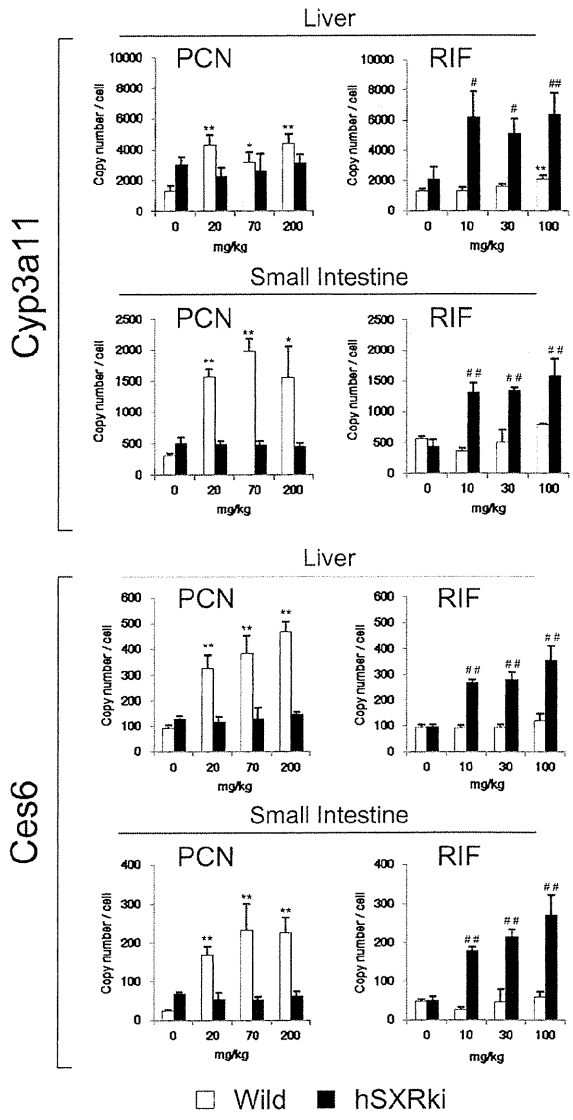

Fig. 3. Humanized response of hSXRki mice to RIF and PCN; Percellome quantitative RT-PCR. WT mice and hSXRki mice (n = 3 each) were singly dosed orally with vehicle (corn oil+0.1% DMSO), 20, 70, or 200 mg/kg PCN, or 10, 30, or 100 mg/kg of RIF (approximately equivalent in molar dose each other). Percellome quantitative RT-PCR data of Cyp3a11 and Ces6, both known as SXR target genes, in liver and small intestinal mucosa showed humanized responses in hSXRki. Bars = S.D., *; $p < 0.05$, **; $p < 0.01$ compared with vehicle group of WT, #; $p < 0.05$, ##; $p < 0.01$ compared with vehicle group of hSXRki. Analyzed by one-way ANOVA followed by Dunnett's post hoc comparison. Level of significance was set at $p < 0.05$.

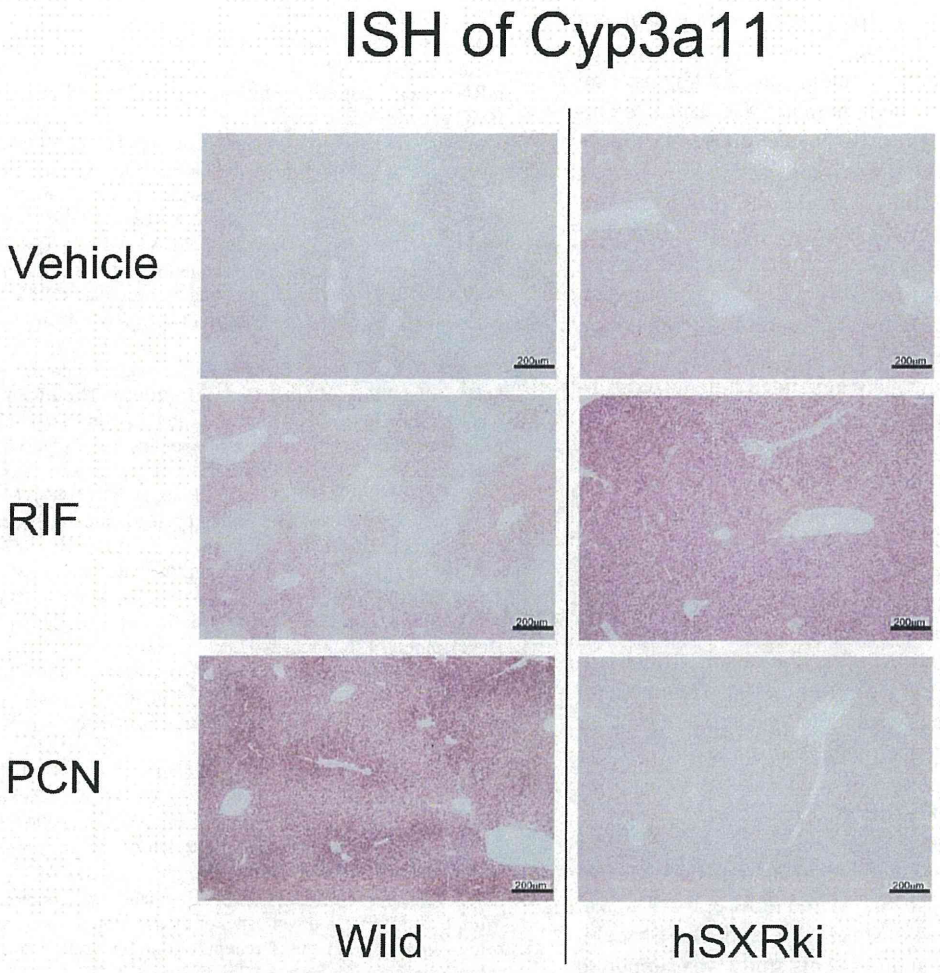

Fig. 4. Humanized response of hSXRki mice to RIF and PCN; *In situ* hybridization for Cyp3a11 mRNA in liver. A DIG-labeled cRNA probe for Cyp3a11 was hybridized and developed for purplish blue chromogenic reaction. Histologically, Cyp3a11 induction was localized around the central veins in both mice with species-specific ligands, respectively.

human-specific ligand RIF to the mice. Induction of the well-known SXR-regulated genes, Cyp3a11 and Ces6 was monitored by Percellome quantitative RT-PCR. As shown in Fig. 3, in the liver and small intestinal mucosa, RIF, but not PCN, induced Cyp3a11 and Ces6 in hSXRki mice (closed column), whereas PCN exclusively induced these genes in WT mice (open column). ISH of Cyp3a11 of the liver also showed humanized responses in hSXRki mice (Fig. 4).

DISCUSSION

We generated a new humanized mouse model in which the ligand binding domain (LBD) of human SXR was homologously knocked-into the murine SXR gene so that systemic response induced by human-selective SXR ligands can be monitored in mice. Firstly, we showed that mRNA from this chimeric gene was expressed at appropriate levels in the same tissues as the endogenous mouse SXR gene in WT mice. Then the humanized response of the mouse was confirmed by monitoring its response to the human-selective activator RIF, and the lack of response to the rodent-selective activator PCN.

There are relatively few reports about the regulation of SXR expression to date. Aouabdi *et al.* (2006) reported the presence of a PPAR alpha binding site 2.2 kb upstream of the transcription start site in human SXR. This site corresponded to the induction site with clofibrate in the rat and they further confirmed its importance using human liver cancer cell line (Huh7). Jung *et al.* (2006) reported the presence of four FXR binding sites in intron 2 of the mouse SXR gene that were required for FXR regulation of SXR expression. This intron 2 region is completely intact in our hSXRki mouse. Therefore, the regulation by FXR should be preserved in our mice.

Compared to the previously generated humanized Alb-SXR, SXR BAC, and hSXR genome mice, we contend that our hSXRki mouse has an advantage because the human-mouse chimeric gene is expressed in the same tissues and at similar levels to endogenous SXR in WT mice under control of the mouse promoter. This feature would make this model suitable not only for systemic toxicity but also toxicity at various stages of development of the embryo and fetus, maturation of infant, and of senescence, where the *cis* and *trans* regulations might be critical in its regulation (Sarsero *et al.,* 2004) (Konopka *et al.,* 2009). Thus, we believe that our system has a broader application range for toxicological studies.

ACKNOWLEDGMENTS

The authors thank Ms. Yuko Matsushima, Mr. Masaki Tsuji, Ms. Maki Otsuka, Mr. Yusuke Furukawa, Mr. Kouichi Morita, Ms. Maki Abe, and Ms. Shinobu Watanabe for technical support. This study was supported in part by the Health Sciences Research Grants H19-Tox-ico-Shitei-001 from the Ministry of Health, Labour and Welfare, Japan.

REFERENCES

Aouabdi, S., Gibson, G. and Plant, N. (2006): Transcriptional regulation of the PXR gene: identification and characterization of a functional peroxisome proliferator-activated receptor alpha binding site within the proximal promoter of PXR. Drug Metab. Dispos., **34**, 138-144.

Bertilsson, G., Heidrich, J., Svensson, K., Asman, M., Jendeberg, L., Sydow-Bäckman, M., Ohlsson, R., Postlind, H., Blomquist, P. and Berkenstam, A. (1998): Identification of a human nuclear receptor defines a new signaling pathway for CYP3A induction. Proc. Natl. Acad. Sci., USA, **95**, 12208-12213.

Blumberg, B., Sabbagh, W.Jr., Juguilon, H., Bolado, J.Jr., van Meter, C.M., Ong, E.S. and Evans, R.M. (1998): SXR, a novel steroid and xenobiotic-sensing nuclear receptor. Genes. Dev., **12**, 3195-3205.

Jung, D., Mangelsdorf, D.J. and Meyer, U.A. (2006): Pregnane X receptor is a target of farnesoid X receptor. J. Biol. Chem., **281**, 19081-19091.

Kanno, J., Aisaki, K., Igarashi, K., Nakatsu, N., Ono, A., Kodama, Y. and Nagao, T. (2006): "Per cell" normalization method for mRNA measurement by quantitative PCR and microarrays. BMC genomics, **7**, 64.

Konopka, G., Bomar, J.M., Winden, K., Coppola, G., Jonsson, Z.O., Gao, F., Peng, S., Preuss, T.M., Wohlschlegel, J.A. and Geschwind, D.H. (2009): Human-specific transcriptional regulation of CNS development genes by FOXP2. Nature, **462**, 213-217.

Lehmann, J.M., McKee, D.D., Watson, M.A., Willson, T.M., Moore, J.T. and Kliewer, S.A. (1998): The human orphan nuclear receptor PXR is activated by compounds that regulate CYP3A4 gene expression and cause drug interactions. J. Clin. Invest., **102**, 1016-1023.

Ma, X., Shah, Y., Cheung, C., Guo, G.L., Feigenbaum, L., Krausz, K.W., Idle, J.R. and Gonzalez, F.J. (2007): The PREgnane X receptor gene-humanized mouse: a model for investigating drug-drug interactions mediated by cytochromes P450 3A. Drug Metab. Dispos., **35**, 194-200.

Saga, Y., Hata, N., Koseki, H. and Taketo, M.M. (1997): Mesp2: a novel mouse gene expressed in the presegmented mesoderm and essential for segmentation initiation. Genes. Dev., **11**, 1827-1839.

Saga, Y., Miyagawa-Tomita, S., Takagi, A., Kitajima, S., Miyazaki, J. and Inoue, T. (1999): MesP1 is expressed in the heart precursor cells and required for the formation of a single heart tube. Development, **126**, 3437-3447.

Sakai, K. and Miyazaki, J. (1997): A transgenic mouse line that retains Cre recombinase activity in mature oocytes irrespective of the cre transgene transmission. Biochem. Biophys. Res. Commun., **237**, 318-324.

Sarsero, J.P., Li, L., Holloway, T.P., Voullaire, L., Gazeas, S., Fowler, K.J., Kirby, D.M., Thorburn, D.R., Galle, A., Cheema, S., Koenig, M., Williamson, R. and Ioannou, P.A. (2004): Human BAC-mediated rescue of the Friedreich ataxia knockout mutation in transgenic mice. Mamm. Genome., **15**, 370-382.

Scheer, N., Ross, J., Rode, A., Zevnik, B., Niehaves, S., Faust, N. and Wolf, C.R. (2008): A novel panel of mouse models to evaluate the role of human pregnane X receptor and constitutive androstane receptor in drug response. J. Clin. Invest., **118**, 3228-3239.

Suzuki, T., Akimoto, M., Mandai, M., Takahashi, M. and Yoshimura, N. (2005): A new PCR-based approach for the preparation of RNA probe. J. Biochem. Biophys. Methods., **62**, 251-258.

Tirona, R.G., Leake, B.F., Podust, L.M. and Kim, R.B. (2004): Identification of amino acids in rat pregnane X receptor that determine species-specific activation. Mol. Pharmacol., **65**, 36-44.

Watkins, R.E., Wisely, G.B., Moore, L.B., Collins, J.L., Lambert, M.H., Williams, S.P., Willson, T.M., Kliewer, S.A. and Redinbo, M.R. (2001): The human nuclear xenobiotic receptor PXR: structural determinants of directed promiscuity. Science, **292**, 2329-2333.

Xie, W., Barwick, J.L., Downes, M., Blumberg, B., Simon, C.M., Nelson, M.C., Neuschwander-Tetri, B.A., Brunt, E.M., Guzelian, P.S. and Evans, R.M. (2000): Humanized xenobiotic response in mice expressing nuclear receptor SXR. Nature, **406**, 435-439.

Yagi, T., Tokunaga, T., Furuta, Y., Nada, S., Yoshida, M., Tsukada, T., Saga, Y., Takeda, N., Ikawa, Y. and Aizawa, S. (1993): A novel ES cell line, TT2, with high germline-differentiating potency. Anal. Biochem., **214**, 70-76.

Zhou, C., Tabb, M.M., Sadatrafiei, A., Grün, F. and Blumberg, B. (2004) Tocotrienols activate the steroid and xenobiotic receptor, SXR, and selectively regulate expression of its target genes. Drug Metab. Dispos., **32**, 1075-1082.

LETTER

doi:10.1038/nature10656

GlcNAcylation of histone H2B facilitates its monoubiquitination

Ryoji Fujiki[1], Waka Hashiba[1], Hiroki Sekine[1], Atsushi Yokoyama[1], Toshihiro Chikanishi[1], Saya Ito[1], Yuuki Imai[1], Jaehoon Kim[2], Housheng Hansen He[3], Katsuhide Igarashi[4], Jun Kanno[4], Fumiaki Ohtake[1], Hirochika Kitagawa[1], Robert G. Roeder[2], Myles Brown[3] & Shigeaki Kato[1,5]

Chromatin reorganization is governed by multiple post-translational modifications of chromosomal proteins and DNA[1,2]. These histone modifications are reversible, dynamic events that can regulate DNA-driven cellular processes[3,4]. However, the molecular mechanisms that coordinate histone modification patterns remain largely unknown. In metazoans, reversible protein modification by *O*-linked *N*-acetylglucosamine (GlcNAc) is catalysed by two enzymes, *O*-GlcNAc transferase (OGT) and *O*-GlcNAcase (OGA)[5,6]. However, the significance of GlcNAcylation in chromatin reorganization remains elusive. Here we report that histone H2B is GlcNAcylated at residue S112 by OGT *in vitro* and in living cells. Histone GlcNAcylation fluctuated in response to extracellular glucose through the hexosamine biosynthesis pathway (HBP)[5,6]. H2B S112 GlcNAcylation promotes K120 monoubiquitination, in which the GlcNAc moiety can serve as an anchor for a histone H2B ubiquitin ligase. H2B S112 GlcNAc was localized to euchromatic areas on fly polytene chromosomes. In a genome-wide analysis, H2B S112 GlcNAcylation sites were observed widely distributed over chromosomes including transcribed gene loci, with some sites co-localizing with H2B K120 monoubiquitination. These findings suggest that H2B S112 GlcNAcylation is a histone modification that facilitates H2BK120 monoubiquitination, presumably for transcriptional activation.

Some nuclear proteins have been shown to be GlcNAcylated by OGT, for example the enzymatic activity of histone H3K4 methyltransferase 5 (MLL5) is modulated by GlcNAcylation[7–9]. To identify chromatin substrates for OGT further, we screened for unknown GlcNAcylated glycoproteins in HeLa cell chromatin. GlcNAcylated proteins were purified by WGA lectin column chromatography and anti-GlcNAc antibody (clone RL2). Liquid chromatography–mass spectrometry (LC–MS)/MS analysis of the fraction revealed 284 factors, including previously reported GlcNAcylated glycoproteins[6,10] (Supplementary Table 1). Among the candidates, the enrichment of nucleosomes was confirmed by silver staining and western blotting (Supplementary Fig. 2), suggesting one or more histone(s) might have been GlcNAcylated. As OGT is the only known nuclear enzyme for protein GlcNAcylation[5], we asked whether histones served as substrates for OGT *in vitro* (Supplementary Fig. 3). H2A and H2B, as well as H2A variants (H2A.X and H2A.Z), but not H3 and H4, appeared to be GlcNAcylated (Fig. 1a). With histone octamers, H2B, but not H2A, appeared to serve as a substrate (Fig. 1b). Likewise, H2B in *Drosophila* histone was also GlcNAcylated (Supplementary Fig. 4), implying that H2B GlcNAcylation is conserved in metazoans.

A quadrupole (Q)-time of flight (TOF) MS assessment of the *in vitro* GlcNAcylated H2B showed that OGT could transfer three GlcNAc moieties to H2B (Supplementary Fig. 5). Electro-transfer-dissociation (ETD)–MS/MS mapped the sites to S91, S112 and S123 (Fig. 1c and Supplementary Fig. 6). Unlike a recent report[11], we were unable to detect the reported sites in H2B S36 and H4 S47. However, H2A T101 was detected as a GlcNAc site when H2A protein alone was used (data not shown). This discrepancy in identified GlcNAc sites might be due to differences in experimental approaches.

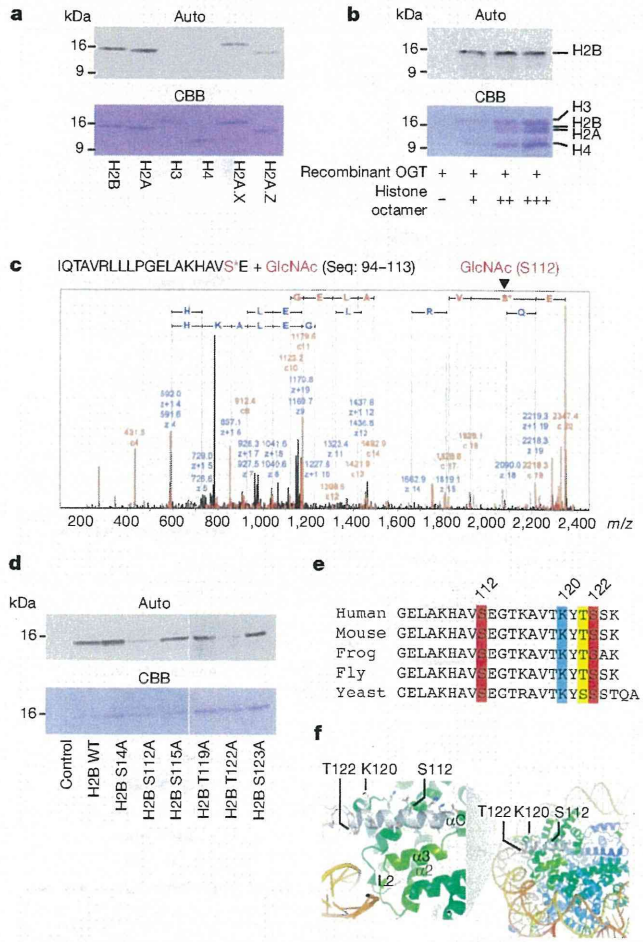

Figure 1 | H2B is GlcNAcylated at the C-terminal S112. **a**, **b**, *In vitro* OGT assay with recombinant histones (**a**) or the octamers reconstituted *in vitro* (**b**). Histones were GlcNAcylated by uridine diphosphate (UDP)-[^{3}H]GlcNAc and OGT, and the radiolabelled histones were subjected to autoradiography (top) and CBB staining (bottom). **c**, ETD–MS/MS scanned the GlcNAcylated peptides (2349.43 *m/z*) in Supplementary Fig. 5b. **d**, A series of H2B mutants at the indicated S/T was assessed by *in vitro* OGT assays. **e**, Sequence alignment of αC. **f**, The locations of the GlcNAc sites and the ubiquitination site of H2B in a nucleosome. The αC helix is illustrated as a white ribbon.

[1]Institute of Molecular and Cellular Biosciences, University of Tokyo, 1-1-1 Yayoi, Bunkyo-ku, Tokyo 113-0032, Japan. [2]Laboratory of Biochemistry and Molecular Biology, The Rockefeller University, New York, New York 10065, USA. [3]Department of Medical Oncology, Dana-Farber Cancer Institute and Harvard Medical School, Boston, Massachusetts 02115, USA. [4]Division of Cellular and Molecular Toxicology, National Institute of Health Sciences, 1-18-1 Kamiyoga, Setagaya-ku, Tokyo 158-8501, Japan. [5]ERATO, Japan Science and Technology Agency, Kawaguchi, Saitama 332-0012, Japan.

Next, *in vitro* OGT assays using peptide arrays covering full-length H2B revealed peaks at 101–115 peptides in the carboxy (C)-terminal α-helix (αC)[12] (Supplementary Fig. 7). This peptide was found to bear only one moiety by matrix-assisted laser desorption/ionization–time of flight (MALDI–TOF)/MS (Supplementary Fig. 8). Indeed, substitutions of S112 and T122 to A significantly reduced *in vitro* GlcNAcylation by OGT (Fig. 1d), but not mutations in the amino (N)-terminal tail (Supplementary Fig. 9). On the basis of these data, we concluded that the conserved S112 was a GlcNAc site in H2B, whereas T122 might be needed for recognition by OGT (Fig. 1e, f).

With our newly developed antibody (Supplementary Fig. 10), H2B S112 GlcNAc was detected in histones of HeLa cells. Depletion of glucose from the media for 24 h induced deglycosylation with neither overt cell death (Fig. 2a and Supplementary Fig. 11) nor alteration in histone acetylation marks of cell state indicators (H3 K14, H3 K56, H4 K16)[13,14] (Supplementary Fig. 12). H2B S112 GlcNAc could be restored by re-treatment with glucose at physiological concentrations (Supplementary Fig. 13).

Because many histone modifications are orchestrated, we tested if H2B S112 GlcNAc influenced H2B K120 monoubiquitination because of their proximity. After glucose depletion, replenishment of glucose gradually increased global GlcNAcylation of proteins, followed by H2B S112 GlcNAc and H2B monoubiquitination (Fig. 2b, c). Their reciprocal modifications disappeared when OGT was knocked down (Fig. 2d and Supplementary Fig. 14). In addition, in the immunoprecipitates of H2B containing the S112A and T122A double mutations (H2B AA), no response of K120 monoubiquitination to extracellular glucose was detected (Fig. 2e and Supplementary Fig. 15). Conversely, GlcNAcylation of H2B S112 was observed, even when K120 was mutated to R (Fig. 2e). From these findings, we conclude that H2B K120 monoubiquitination is mediated, at least in part, through S112 GlcNAcylation.

As glucosamine, but not pyruvate, potentiated H2B S112 GlcNAc (Fig. 2f), it appeared that this GlcNAcylation step was dependent on the HBP. To clarify this point, two HBP inhibitors (DON and AZA) were tested (Supplementary Information). After glucose depletion from media, these inhibitors attenuated the effect of glucose in H2B S112 GlcNAcylation along with K120 monoubiquitination (Fig. 2f).

In yeast, it was previously shown that H2B K120 monoubiquitination was induced by carbohydrates by glycolysis[15]. To address this issue, inhibitors of both glycolysis and deGlcNAcylation were applied to assess the crosstalk between the two modifications. When the cells were treated with iodoacetate, which blocks glycolysis but not HBP[15], the glucose effects on histone modifications were impaired, whereas the additional treatment of an OGA inhibitor (PUGNAc) restored both H2B S112 and K120 monoubiquitination (Supplementary Fig. 16). These data support the notion that H2B S112 GlcNAc senses decreases in glucose levels below normal levels and acts to promote H2B monoubiquitination, a modification that is associated with active transcription. Together with the fact that OGT is absent in yeast[6], the present H2B S112 GlcNAc-dependent pathway appears to constitute a system capable of sensing nutritional states in metazoans.

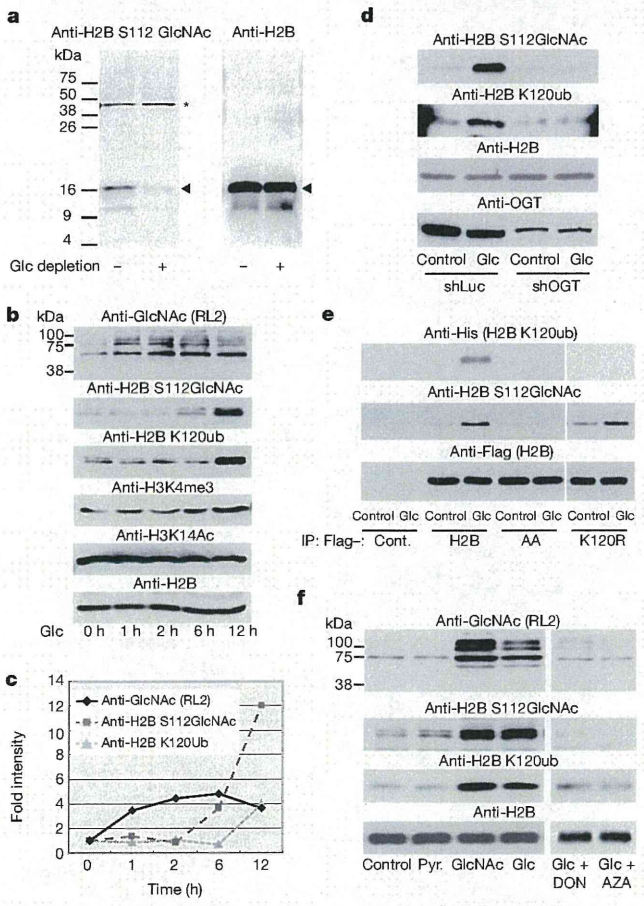

Figure 2 | H2B S112 GlcNAc is a glucose-responsive modification linked to K120 monoubiquitination (ub). **a**, Chromatin was prepared from HeLa cells cultured in media with or without 1 $g l^{-1}$ glucose (Glc) for 24 h, and subjected to western blotting. Arrowheads show the indicated proteins. Asterisks indicate non-specific band. **b**, **c**, After 24 h Glc depletion, chromatin samples were prepared from HeLa cells treated with 4.5 $g l^{-1}$ Glc for the indicated time. The intensities of the western blotting bands (**b**) were quantified (**c**). **d**, **e**, The effects of OGT knockdown (**d**) or H2B mutations (**e**) on H2B modifications after Glc replenishment. **f**, Western blotting analysis of the H2B modifications in HeLa cells that were cultured in DMEM without Glc (Cont.), or supplemented with 1 mM pyruvate (Pyr.), 10 mM GlcNAc or 4.5 $g l^{-1}$ Glc with or without HBP inhibitors, 6-diazo-5-oxo-L-norleucine (100 μM, DON) or azaserine (100 μM, AZA).

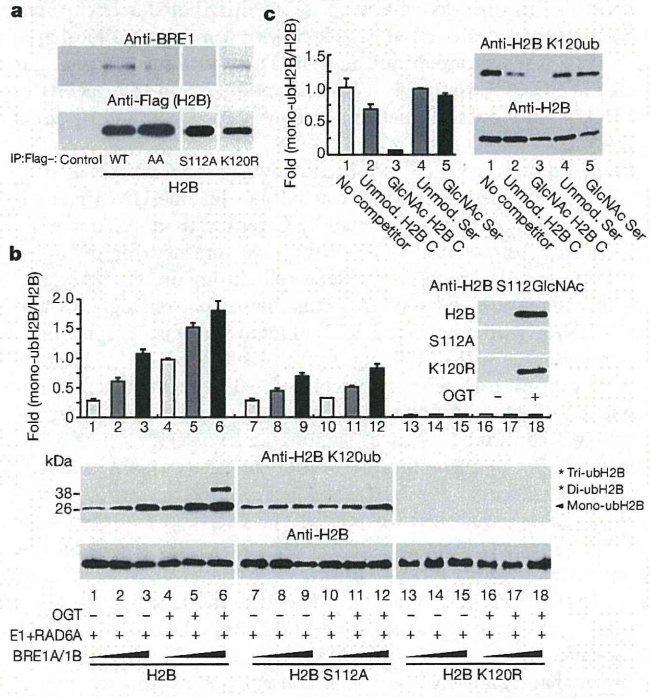

Figure 3 | GlcNAcylation at S112 facilitates ubiquitination at K120 in H2B. **a**, Western blotting analysis of the interaction of H2B mutants with BRE1A. **b**, **c**, *In vitro* monoubiquitination assay with GlcNAcylated H2B (**b**), or in the presence of competitor peptides (**c**). H2B was GlcNAcylated *in vitro* (**b**, top right), and the reactants were subsequently ubiquitinated by H2B monoubiquitination ligase. The reaction was performed with the indicated competitor peptides (0.25 μg ml^{-1}) (**c**). H2B K120 monoubiquitination was detected by western blotting (**b**, bottom; **c**, right) and quantified (**b**, top; **c**, left). Error bars, means and s.d. ($n = 3$).

The terminal GlcNAc of polysaccharides reportedly serves as a recognition moiety for E3 monoubiquitination ligase[16]. Therefore, we proposed that H2B S112 GlcNAc affected K120 monoubiquitination by the BRE1A/1B complex[17]. Flag-tagged H2B, but not AA or S112A, was co-immunoprecipitated with BRE1A (Fig. 3a). This association was observed in the presence of physiological levels of glucose in the media, and BRE1A was bound to H2B S112 GlcNAc (Supplementary Fig. 17). We then assessed how the GlcNAcylation of H2B influenced its *in vitro* ubiquitination by E1, RAD6A (E2) and the BRE1A/1B complex (E3). Although H2B K120 could be substantially ubiquitinated only by the ligases (Supplementary Fig. 18), GlcNAcylation of H2B promoted subsequent H2B ubiquitination, but not its S112A mutant (Fig. 3b). Likewise, ubiquitination was significantly attenuated by the presence of an H2B-S112-GlcNAcylated peptide, but not by either the unmodified control peptide or by GlcNAcylated serine (Fig. 3c). On the basis of these results, we conclude that the GlcNAc moiety at H2B S112 may anchor H2B monoubiquitination ligase.

To illustrate the role of H2B S112 GlcNAc in chromatin regulation, its location was visualized on fly polytene chromosomes. H2B S112 GlcNAc was detected widely in euchromatin, and, as anticipated, its signal disappeared in an OGT-disrupted fly, sxc^{1}/sxc^{78} (Supplementary Fig. 19). H2B S112 GlcNAc overlapped with H3K4 me2 more than with H3K9 me2 or H3K27 me3 (Fig. 4a). Similarly, in immunostained HeLa cells, H2B S112 GlcNAc sites appeared exclusively in 4′,6-diamidino-2-phenylindole (DAPI)-poor areas (Supplementary Fig. 20). Thus, H2B S112 GlcNAc probably accumulates in active chromatin rather than inactive chromatin.

To determine the precise loci of H2B S112 GlcNAc in HeLa cells, we performed chromatin immunoprecipitation (ChIP) and high-throughput sequencing (ChIP-seq). We confirmed ChIP quality by enrichments of H2B GlcNAc as well as H3K4 me2 and H2B K120 monoubiquitination, but neither H3K9 me2 nor H3K27 me3 (Supplementary Fig. 21). A total of 47,375 peaks were found widely distributed over the genome (Supplementary Fig. 22). However, H2B S112 GlcNAc peaked near transcription start sites (TSS), whereas the distribution decreased at transcription termination sites (TTS) (Fig. 4b), suggesting that it correlated with transcriptional regulation. To test this assumption, the activities of genes harbouring H2B S112 GlcNAc near TSS were estimated by microarray analysis (Supplementary Table 2). The average profiles near TSS significantly correlated with gene activity (Fig. 4c). Moreover, the expression levels of the 1,299 genes were reliably measured, and 1,021 genes showed high expression (Supplementary Fig. 23a and Supplementary Table 3b). Moreover, gene ontology analysis revealed that there was an association of the genes harbouring H2B S112 GlcNAc to cellular metabolic processes (Supplementary Fig. 23b and Supplementary Table 3c).

Next, we analysed the genome-wide overlap of H2B S112 GlcNAc with K120 monoubiquitination. A total of 44,158 peaks of H2B K120 monoubiquitination were detected, and their average profiles near TSS were similar to those profiles of H2B S112 GlcNAc (Supplementary

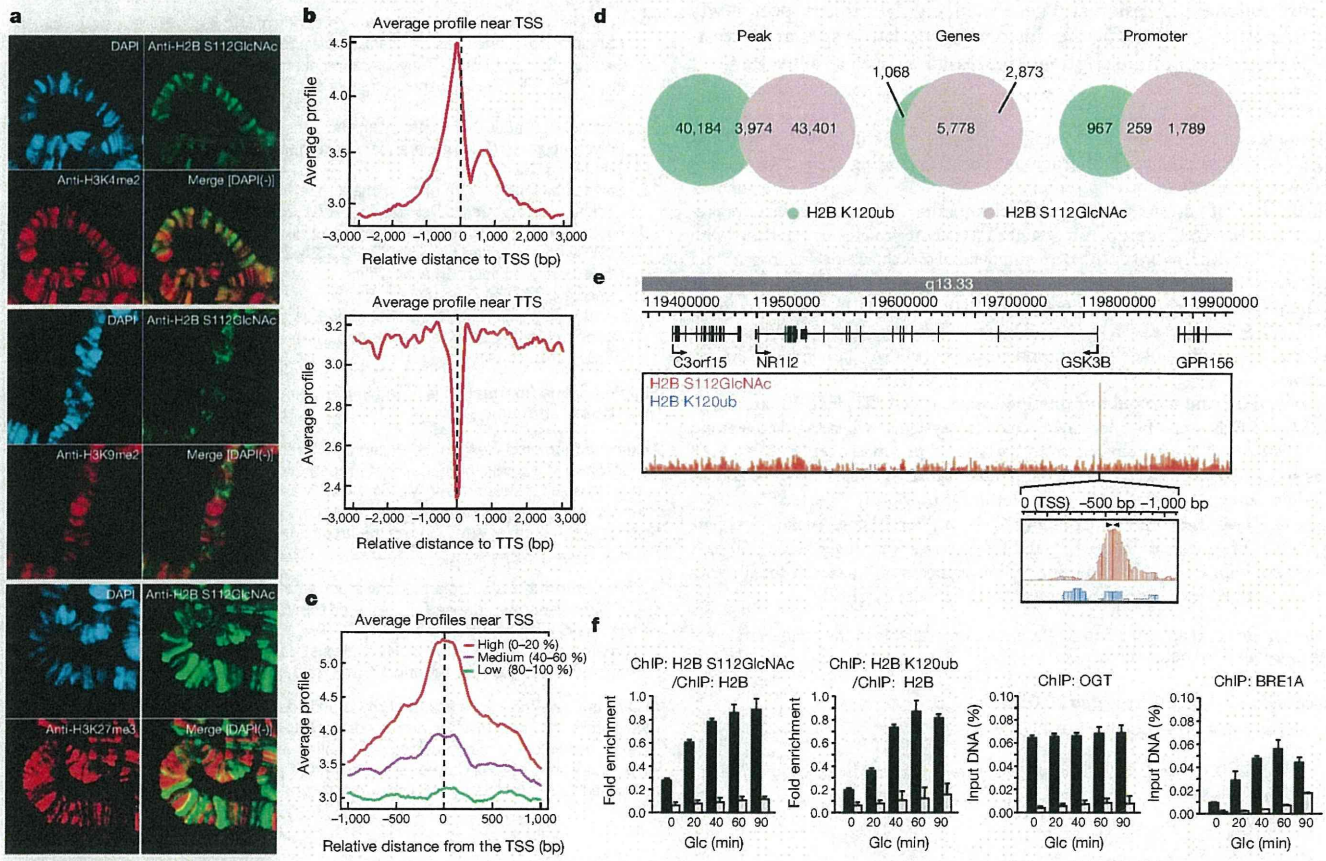

Figure 4 | GlcNAcylated H2B is associated with transcribed genes. **a**, Polytene staining with α-H2B S112 GlcNAc (green) and DAPI (blue) along with α-H3K4me2 (red, top), α-H3K9me2 (red, middle) or α-H3K27me3 (red, bottom). **b–e**, ChIP-seq analysis of the H2B S112 GlcNAc and K120 monoubiquitination. The distributions of H2B S112 GlcNAc were averaged near TSS (top) and TTS (bottom) (**b**). The average profiles of H2B S112 GlcNAc near TSS were calculated based on the associated gene activities (**c**). Venn diagrams showing overlap of the peaks (**d**, left), and the genes (**d**, middle) and the promoter (**d**, right) harbouring the modifications. The ChIP-seq profile surrounding the *GSK3B* gene (**e**). Arrowhead, position of qPCR primer. **f**, ChIP–qPCR validation in the GSK3B promoter. After Glc depletion, the control HeLa cells (black bar) and the OGT-knockdown cells (white bar) were replenished with Glc for 24 h. Then, the cells were subjected to ChIP with the indicated antibody and qPCR analysis. Error bars, means and s.d. ($n = 3$).

Fig. 24). Among the H2B K120 monoubiquitination peaks, nearly 10% (3,974 peaks) overlapped with H2B S112 GlcNAc peaks (Fig. 4d, left), and this evaluation was confirmed by a sequential ChIP–reChIP assay (Supplementary Fig. 25). Although 5,778 genes (66.8% of H2B S112 GlcNAc and 84.4% of K120 monoubiquitination) were found at the same loci (Fig. 4d, middle, and Supplementary Table 3d), 259 genes were identified when the two peaks were compared only within the promoters (Fig. 4d, right). The results of the ChIP-seq analysis were validated by ChIP–quantitative PCR (qPCR) assessment for the glycogen synthase kinase 3β (*GSK3B*) gene (Fig. 4e, f). These findings suggest that at several H2B S112 GlcNAc sites, it aids H2B monoubiquitination ligase recruitment whereas at others additional or different factors may be operational.

Here we provide evidence that histone GlcNAcylation is a post-translational modification correlated with active transcriptional events, and is responsive to serum glucose levels and/or cellular energy states in certain cell types (Supplementary Fig. 1). Using an antibody that specifically recognizes the S112 GlcNAc moiety of endogenous H2B, H2B was shown to serve as an OGT substrate. We have focused on the role of H2B S112 GlcNAcylation in gene regulation (Supplementary Fig. 1). Genome-wide analysis revealed that H2B S112 GlcNAc was frequently located near transcribed genes, suggesting that histone GlcNAcylation facilitates transcription of the genes. This idea is supported by previous reports that transcriptional output driven by several transcription factors is co-activated by OGT[9,18–20]. However, recent papers reported that *Drosophila* OGT is itself a polycomb group protein[8,21], and that many *O*-GlcNAcylated factors are involved in transcriptional repression and gene silencing[7,8]. In this respect, it will be interesting to identify other histone glycosylation sites and investigate their roles in transcriptional repression as well as activation.

METHODS SUMMARY

Plasmids and cell culture. All plasmids were generated with standard protocols (see Methods). Retrovirus production, infection and sorting of the infected cells followed previously reported protocols[9].

Purification of GlcNAc proteins from chromatin. Chromatin pellets were prepared from HeLa cells as previously described[22]. GlcNAc proteins were enriched with α-*O*-GlcNAc (RL2) antibody (Abcam) immobilized on Dynabeads (Invitrogen), and released with GlcNAc-*O*-serine.

Generation of monoclonal antibody. The synthetic H2B S112 GlcNAc peptide (CKHAV S(GlcNAc) EGTK) was used to immunize mice. The hybridomas were selected by enzyme-linked immunosorbent assay (ELISA) and western blotting analysis.

***In vitro* OGT and monoubiquitination assays.** Flag–OGT, Flag–E1, and Flag–BRE1A/BRE1B were purified by baculoviral systems, whereas histones and 6 × His-RAD6A were prepared from bacteria as previously reported[17,23]. H2B was incubated with OGT or H2B monoubiquitination ligases *in vitro*, and its modification was detected by western blotting as previously reported[9,23].

ChIP-seq and ChIP–qPCR. ChIP and ChIP-seq library construction was performed as previously described[24,25], and the libraries were sequenced to 50 base pairs (bp) with Hiseq2000 (Illumina). The fragments of interest in the libraries were quantified with specific promoter sets (Methods) by qPCR.

Full Methods and any associated references are available in the online version of the paper at www.nature.com/nature.

Received 16 July 2010; accepted 20 October 2011.
Published online 27 November 2011.

1. Strahl, B. D. & Allis, C. D. The language of covalent histone modifications. *Nature* **403,** 41–45 (2000).
2. Kouzarides, T. Chromatin modifications and their function. *Cell* **128,** 693–705 (2007).
3. Li, B., Carey, M. & Workman, J. L. The role of chromatin during transcription. *Cell* **128,** 707–719 (2007).
4. Berger, S. L. The complex language of chromatin regulation during transcription. *Nature* **447,** 407–412 (2007).
5. Hart, G. W., Housley, M. P. & Slawson, C. Cycling of O-linked β-*N*-acetylglucosamine on nucleocytoplasmic proteins. *Nature* **446,** 1017–1022 (2007).
6. Love, D. C. & Hanover, J. A. The hexosamine signaling pathway: deciphering the 'O-GlcNAc code'. *Sci. STKE* **2005,** re13 (2005).
7. Yang, X., Zhang, F. & Kudlow, J. E. Recruitment of O-GlcNAc transferase to promoters by corepressor mSin3A: coupling protein O-GlcNAcylation to transcriptional repression. *Cell* **110,** 69–80 (2002).
8. Gambetta, M. C., Oktaba, K. & Muller, J. Essential role of the glycosyltransferase sxc/Ogt in polycomb repression. *Science* **325,** 93–96 (2009).
9. Fujiki, R. *et al.* GlcNAcylation of a histone methyltransferase in retinoic-acid-induced granulopoiesis. *Nature* **459,** 455–459 (2009).
10. Wang, Z. *et al.* Extensive crosstalk between O-GlcNAcylation and phosphorylation regulates cytokinesis. *Sci. Signal.* **3,** ra2 (2010).
11. Sakabe, K., Wang, Z. & Hart, G. W. β-N-acetylglucosamine (O-GlcNAc) is part of the histone code. *Proc. Natl Acad. Sci. USA* **107,** 19915–19920 (2010).
12. Luger, K. *et al.* Crystal structure of the nucleosome core particle at 2.8 Å resolution. *Nature* **389,** 251–260 (1997).
13. Das, C., Lucia, M. S., Hansen, K. C. & Tyler, J. K. CBP/p300-mediated acetylation of histone H3 on lysine 56. *Nature* **459,** 113–117 (2009).
14. Dang, W. *et al.* Histone H4 lysine 16 acetylation regulates cellular lifespan. *Nature* **459,** 802–807 (2009).
15. Dong, L. & Xu, C. W. Carbohydrates induce mono-ubiquitination of H2B in yeast. *J. Biol. Chem.* **279,** 1577–1580 (2004).
16. Yoshida, Y. *et al.* E3 ubiquitin ligase that recognizes sugar chains. *Nature* **418,** 438–442 (2002).
17. Kim, J. *et al.* RAD6-Mediated transcription-coupled H2B ubiquitylation directly stimulates H3K4 methylation in human cells. *Cell* **137,** 459–471 (2009).
18. Dentin, R. *et al.* Hepatic glucose sensing via the CREB coactivator CRTC2. *Science* **319,** 1402–1405 (2008).
19. Chikanishi, T. *et al.* Glucose-induced expression of MIP-1 genes requires O-GlcNAc transferase in monocytes. *Biochem. Biophys. Res. Commun.* **394,** 865–870 (2010).
20. Jackson, S. P. & Tjian, R. O-glycosylation of eukaryotic transcription factors: implications for mechanisms of transcriptional regulation. *Cell* **55,** 125–133 (1988).
21. Sinclair, D. A. *et al. Drosophila* O-GlcNAc transferase (OGT) is encoded by the Polycomb group (PcG) gene, super sex combs (sxc). *Proc. Natl Acad. Sci. USA* **106,** 13427–13432 (2009).
22. Sawatsubashi, S. *et al.* A histone chaperone, DEK, transcriptionally coactivates a nuclear receptor. *Genes Dev.* **24,** 159–170 (2009).
23. Fujiki, R. *et al.* Ligand-induced transrepression by VDR through association of WSTF with acetylated histones. *EMBO J.* **24,** 3881–3894 (2005).
24. He, H. H. *et al.* Nucleosome dynamics define transcriptional enhancers. *Nature Genet.* **42,** 343–347 (2010).
25. Minsky, N. *et al.* Monoubiquitinated H2B is associated with the transcribed region of highly expressed genes in human cells. *Nature Cell Biol.* **10,** 483–488 (2008).

Supplementary Information is linked to the online version of the paper at www.nature.com/nature.

Acknowledgements We thank A. Miyajima, S. Saito and N. Moriyama for experimental support, and M. Yamaki for manuscript preparation. We also thank Y. Maekawa, J. Seta and N. Iwasaki for support with MS. This work was supported in part by The Naito Foundation, the Astellas foundation (to R.F.), the Ministry of Education, Culture, Sports, Science and Technology (MEXT) and the Japan Society for the Promotion of Science (to R.F. and S.K.).

Author Contributions S.K. planned the study with H.K.; R.G.R. and M.B. provided support and general guidance; R.F. designed the study and performed the experiments with H.S. (α-*O*-GlcNAc purification), A.Y. (LC–MS/MS), W.H. (*O*-GlcNAc site mapping), T.C. (*in vitro* OGT assay), S.I. (*Drosophila* analysis), Y.I., H.H.H. (ChIP-seq), F.O., J.K. (*in vitro* monoubiquitination assay), K.I. and J.K (microarray).

Author Information Reprints and permissions information is available at www.nature.com/reprints. The authors declare no competing financial interests. Readers are welcome to comment on the online version of this article at www.nature.com/nature. Correspondence and requests for materials should be addressed to S.K. (uskato@mail.ecc.u-tokyo.ac.jp).

METHODS

Plasmids and retroviruses. Complementary DNAs (cDNAs) of N-terminally Flag-tagged H2B and its mutant were subcloned into pcDNA3 (Invitrogen). A series of H2B point mutants were subcloned into the pET3 vector (Novagen). shRNA sequences targeting hOGT (5′-GCACATAGCAATCTGGCTTCC-3′) and *Renilla* luciferase (5′-TGCGTTGCTAGTACCAAC-3′, as a control) were inserted into the pSIREN-RetroQ-ZsGreen vector (Clontech). For retroviral production, the constructed shRNA vectors were transfected into PLAT-A cells. The virus contained in the medium was used for infection.

Generation of stable cell lines. To generate OGT-KD cells by retroviral infection, 10^6 cells were plated in 60 mm culture dishes, treated with 3 ml of retroviral cocktail (1 ml of the prepared retroviral solution plus 2 ml of DMEM with 10% FBS and 8 μg ml^{-1} polybrene), then cultured for another 48 h. A FACSVantage (BD) sorter was used to isolate the retrovirally transduced, enhanced green fluorescent protein (eGFP)-positive cells, as previously described[9]. To generate the cells stably expressing Flag-tagged constructs, HeLa cells were transfected with the pcDNA vectors encoding the Flag-tagged H2B or the AA mutant. The cells containing the integrated vectors were selected by exposure to 0.5 mg ml^{-1} G418.

Generation of monoclonal antibody. H2B S112 GlcNAc peptide (CKHAV S(GlcNAc) EGTK) was synthesized (MBL Institute) and used as an antigen (Operon Biotechnologies). The hybridomas were briefly screened using ELISA with the GlcNAc peptide, and finally selected by immunoblot analysis with the *in vitro* GlcNAcylated H2B.

Antibodies. Antibodies were obtained as follows: α-Flag M2 agarose (Sigma), α-H2A, α-H2B, α-H3, α-H4 (Abcam), α-H2B K120 monoubiquitination (Upstate), α-GlcNAc (RL2 or CTD110.6) (Abcam), α-OGT (Sigma), α-Flag (Sigma) and α-RNF20/BRE1A (Bethyl).

Purification and identification of GlcNAc proteins. The α-*O*-GlcNAc-immobilized beads were prepared with 15 μg α-*O*-GlcNAc (RL2) antibody and 0.5 ml of Dynabeads M-280 sheep α-mouse IgG (Invitrogen) according to the manufacturer's instructions. Chromatin extracts from HeLa cells (0.5 g protein) were prepared essentially as previously described[22]. In brief, the chromatin pellet, which consisted of residual material from the nuclear extract preparation with buffers supplemented with 1 mM streptozotocin (STZ), was re-suspended with micrococcal nuclease (MNase) buffer (20 mM Tris-HCl, 1 mM $CaCl_2$, 2 mM $MgCl_2$, 0.1 M KCl, 0.1% (v/v) Triton-X, 0.3 M sucrose, 1 mM DTT, 1 mM benzamidine, 0.2 mM PMSF, 1 mM STZ, pH 7.9). After addition of 3 U ml^{-1} MNase, the samples were incubated for 30 min at room temperature with continuous homogenization and the reaction was stopped by adding 5 mM EGTA and 5 mM EDTA. After centrifugation at 2,000*g* for 30 min at 4 °C, the supernatant (chromatin extract) was used for the following purification steps. The chromatin extracts were passed through a WGA agarose column (Vector). The flow-through fraction was further mixed with α-*O*-GlcNAc-immobilized beads and rotated for 8 h at 4 °C. After three washes with buffer D (20 mM Tris-HCl, 0.2 mM EDTA, 5 mM $MgCl_2$, 0.1 M KCl, 0.05% (v/v) NP-40, 10% (v/v) glycerol, 1 mM DTT, 1 mM benzamidine, 0.2 mM PMSF, 1 mM STZ, pH 7.9), glycoproteins were eluted twice with buffer D plus 0.4 mg ml^{-1} GlcNAc-*O*-serine (MBL) (elutions 1 and 2) and finally with 0.1 M glycine-HCl (pH2.0) (elution 3). Eluted proteins were desalted by methanol–chloroform precipitation, digested with trypsin (Promega) then loaded on the automated LC–MS/MS system, which was assembled with Zaplous nano-LC (AMR) plumbed with a reverse-phase C18 electrospray ionization (ESI) column (LC assist) and a Fiinigan LTQ ion-trap mass spectrometer (Thermo). The LC–MS/MS data were processed using Thermo BioWorks (Thermo) and SEQUEST (Thermo) for protein identification. The list of the identified proteins was further analysed by using the 'gene functional classification tool' in DAVID bioinformatics resources 6.7 (http://david.abcc.ncifcrf.gov/).

Recombinant proteins. Preparation of recombinant proteins was performed as previously reported[9,23]. Recombinant Flag–OGT, Flag–E1, Flag–BRE1A/B complexes were isolated by baculovirus expression and immunoprecipitation-based purification with α-Flag M2 agarose (Sigma). Recombinant 6 × His-RAD6A was expressed in bacteria and partly isolated with a HIS-Select Nickel Affinity Gel (Sigma). The eluate was diluted 1:20 with BC0 (20 mM HEPES, 0.2 mM EDTA, 10% (v/v) glycerol, pH 7.9), and fractionated with a Resource Q column (GE Healthcare) using a linear gradient (0–0.5 M KCl) method. Preparation of recombinant *Xenopus* histone H2B and its mutants was performed as previously described[9,23].

***In vitro* GlcNAcylation assay (autoradiographic analysis).** Recombinant Flag–OGT protein (0.5 μg) was incubated with 0.5 μg of recombinant histone and 0.2 mM (0.2 μCi) UDP-[^{3}H]GlcNAc (PerkinElmer) in a 25 μl reaction (50 mM Tris-HCl, 12.5 mM $MgCl_2$, 1 mM DTT, pH 7.5) for 24 h at 37 °C. The reaction was resolved with SDS–PAGE, blotted onto a polyvinylidene difluoride (PVDF) membrane, then subjected to autoradiography after spraying EN^{3}HANCE (NEN Lifescience).

***In vitro* GlcNAcylation assay (MS analysis).** Recombinant histones (1 μg) or recombinant histone octamers assembled *in vitro* (1 μg) were GlcNAcylated by recombinant Flag–OGT in 25 μl reactions (50 mM Tris-HCl, 2 mM UDP-GlcNAc, 12.5 mM $MgCl_2$, 1 mM DTT, pH 7.5) for 24 h at 37 °C. The reactions were directly subjected to a nano-LC ESI–TOF mass spectrometer system, which was assembled with a 1100 nanoLC (Agilent) plumbed with a ZORBAX 300SB-C18 column (Agilent) and micrOTOF (Bruker). Or, the reactions were digested with trypsin (Promega) and subjected to purification of glycopeptides with an MBLAC WGA kit (Bruker). The enriched glycopeptides were loaded on the nano-LC ESI–ETD ion-trap mass-spectrometer system, which was assembled with the Agilent HP1200 Nano (Agilent) plumbed with ZORBAX 300SB-C18 (Agilent) and amaZon ETD (Bruker).

***In vitro* monoubiquitination assay.** GlcNAcylated histones (1 μg) were ubiquitinated with the E1 (0.1 μg), RAD6 (0.2 μg), BRE1 complex (0.5 μg), ubiquitin (3 μg) in 50 mM Tris (pH7.9), 5 mM $MgCl_2$, 4 mM ATP at 37 °C for 24 h.

ChIP-seq and ChIP–qPCR. ChIP and ChIP-seq libraries were constructed as previously described[24,25]. For ChIP-seq analysis, the libraries were sequenced to 50 bp with Hiseq2000 (Illumina). For ChIP–qPCR analysis, the fragments of interest in the libraries were quantified with Thermal Cycler TP800 (TAKARA) and SYBR Premix Ex Taq II (Takara). The qPCR primer sets for the *GSK3B* gene were 5′-TGCAAGCTCTCAGACGCTAA-3′ and 5′-CTCATTTCTCATGGGCG TTT-3′.